COBEM 2021 26th International Congress of Mechanical Engineering
ABCM Associação Brasileira de Engenharia e Ciências Mecânicas
November 22-26, 2021, Virtual Congress, Brazil

COB-2021-1605 CFD ESTIMATION OF SAFETY DISTANCES FROM POOL FIRES

Marcelo André Cordeiro da Silva
Norberto Mangiavacchi
Rio de Janeiro State University, Rio de Janeiro, RJ, Brazil
silva.marceloac@gmail.com, norberto.mangiavacchi@eng.uerj.br

Abstract. *The storage of liquid fuels in aboveground storage tanks is a typical activity in oil refineries and in fuel terminals, with gasoline being one of the most used fuels. This kind of storage offers a risk of fire due to tank leakage, which can cause pool fire, flash fire and fireball. In this paper the heat flux due to thermal radiation caused by pool fire due to leakage of gasoline is analyzed. The pool fire modeling and radiative heat flux calculation as a function of the fire distance were performed by Computational Fluid Dynamics (CFD) using Fire Dynamics Simulator (FDS) and Pyrosim, a graphical user interface for FDS. In this paper, three basic pool fire models are studied: without a tank, with horizontal and with vertical tank. For each model two simulations were performed, one not considering wind and another considering wind. This paper aims to determine the safety distances from pool fires. Distances from pool fire considering impact of the heat flux by radiation on human are found for, where radiative heat flux is 5 kW/m^2 (capable of causing second degree burn) and where radiative heat flux cause death probability of 1%. Safety distance curves were determined.*

Keywords: *CFD, FDS, pool fire, Pyrosim, radiative heat flux modeling.*

1. INTRODUCTION

Oil refineries and fuel terminals store large amount of fuel to send to fuel distributors and gas stations. In these cases, aboveground storage tanks (ASTs) is the most used way to store fuels. These ASTs are normally located in a containment basin to avoid soil contamination in case of fuel tank leakage. A containment basin must have the capacity to contain, without spillage, all the volume of liquid from the tank(s) in case of liquid leakage.

When a leakage in a tank with liquid fuel occurs, the fuel will be exposed in the containment basin. This fuel, in contact with environmental air and certain level of heat, can be ignited causing fire. The fire in the containment basin is classified as a pool fire. In a pool fire, convection currents act shaping the flame, under the influence of turbulence factors. A fraction of the heat generated is emitted in the form of thermal radiation. The impact of this radiative heat flux in a body is greatly influenced by the geometric relationship between the flame and the irradiated body.

When an human body is the receptor from a fire radiative heat flux, certain level of radiation can cause 1st, 2nd or 3rd degree burns, causing minor, moderate or severe injuries or even death (Niazi *et al.*, 2016). A risk analysis that has a pool fire scenario usually takes into account the value of second degree burn (5 kW/m^2), and the radiation values to probabilities of death calculated through probit functions.

There are different types of approaches to prevent human injury due to fire. TNO (VROM, 2005b) presents three classes of mathematical tools for predicting the heat flux at a distance, associated with pool fires on land, they are: semi-empirical models, field models and integral models.

Semi-empirical models are built with relatively simple techniques, where models are designed only to predict quantities such as flame shape and radiative heat flux, rather than to provide a detailed description of the fire itself. There are two types of semi-empirical models: point source models, that assume that the source of the heat radiation is a point, and surface emitter models, which assumes that heat is radiated from the surface of a solid object (usually an inclined cone or cylinder). Semi-empirical models depend heavily on experimental data and correlations for modeling fire shape or center line and are readily embodied in simpler computer programs with short run times.

Field models are based on solutions of the time-averaged Navier-Stokes equations of fluid flow that describe, in partial differential form, the conservation of mass, momentum and scalar quantities in flowing fluid. Field models are mathematically complex, embodied in large computer programs and have significant run times.

Integral models are between semi-empirical models and field models and formulated mathematically in the same way as field models and can in principle contain sub-models of turbulence structure and combustion and heat transfer process. In integral models, equations that describe the conservation of mass, momentum and scalar quantities within a flow are expressed in simplified form, which requires for their solution far less computer time than field models.

2. METHODOLOGY

The methodology applied in this study consists in simulate pool fire scenarios to analyse and predict safety distances using Computation Fluid Dynamics (CFD). For this study it was used CFD program Fire Dynamics Simulator (FDS); Smoke View (SMV), a program used to view FDS simulations; Pyrosim, a graphical user interface for FDS and Smoke View and; Matlab. Some FDS simulation results were used to compute and plot, using Matlab, safety distance values and curves from the fire. This methodology was used by (Silva and Mangiavacchi, 2019) to predict safety distances from Diesel oil pool fires but employing a different methodology to determine radiative heat flux from fire.

In this work, six pool fire cases were modeled and simulated with gasoline fuel:

1. Case 1 - pool fire in a containment basin with a horizontal cylindrical tank and without wind;
2. Case 2 - pool fire in a containment basin with a horizontal cylindrical tank and with wind;
3. Case 3 - pool fire in a vertical cylindrical tank without wind;
4. Case 4 - pool fire in a vertical cylindrical tank with wind;
5. Case 5 - pool fire in a containment basin without tank and without wind and;
6. Case 6 - pool fire in a containment basin without tank and with wind.

The six case studies were simulated during 60 seconds fire since ignition.

2.1 Computational Fluid Dynamics (CFD)

The simulations were performed using Computional Fluid Dynamics (CFD). The CFD software used was Fire Dynamics Simulator (FDS) developed by the National Institute of Standards and Technology (NIST) from US Department of Commerce and VTT Technical Research Centre of Finland. FDS is a CFD model of fire-driven fluid flow that solves numerically a form of the Navier-Stokes equations appropriate for low-speed, thermally-driven flow with an emphasis on smoke and heat transport from fires. The computation can either be treated as a Direct Numerical Simulation (DNS) or as a Large Eddy Simulation (LES). The choice between DNS or LES to model combustion in FDS depends on the resolution of the underlying grid. The simulations presented in this work were performed by LES. The same simulations performed by DNS would require very small grid cells and huge computational demand.

The six models were designed using Pyrosim, a graphical user interface software for FDS that allows to quickly create and manage the details of complex fire models.

2.1.1 Mathematical model

The FDS mathematical models include hydrodynamic model (McGrattan *et al.* 2018a and McGrattan *et al.* 1998), combustion model and thermal radiation model to simulate fire (Hostikka *et al.* 2003 and McGrattan *et al.* 2018a). Probit model equation (VROM, 2005a) was applied to find safety distance relative to 1% probality of human death due to thermal radiation from fire.

2.1.2 Hydrodynamic model

$$\frac{\partial \rho}{\partial t} + \nabla \cdot \rho \mathbf{u} = 0 \tag{1}$$

$$\rho \left(\frac{\partial \mathbf{u}}{\partial t} + \frac{1}{2} \nabla |\mathbf{u}|^2 - \mathbf{u} \times \omega \right) + \nabla p - \rho \mathbf{g} = \nabla \cdot \sigma \tag{2}$$

$$\rho c_p \left(\frac{\partial T}{\partial t} + \mathbf{u} \cdot \nabla T \right) - \frac{dp_0}{dt} = \dot{q} + \nabla \cdot k \nabla T \tag{3}$$

$$p_0(t) = \rho R T, \tag{4}$$

where, ρ is density; $\mathbf{u}$ is the velocity vector; ω is the vorticity; p_0 is the average pressure; $\mathbf{g}$ is the gravity acceleration; c_p is the specific heat at constant pressure; T is the absolute temperature; k is the thermal conductivity; t is time; $\dot{q}$ is the volumetric heat released; R is the gas constant and σ is the standard stress tensor for compressible fluids.

2.1.3 Combustion model

$$\dot{q}_c'' = \Delta H_o \frac{dY_o}{dZ}(\rho D)\nabla Z \cdot \mathbf{n}; Z < Z_f, \tag{5}$$

where, $\dot{q}_c''$ is the heat release rate per unit area of flame surface; ΔH_o is the energy released per unit mass of oxygen consumed, being almost constant for a wide range of fuels; **n** is the unit normal facing outward from the fuel; Z is the mixture fraction of air and fuel; Z_f is this mixture fraction limit to combustion; dY_o/dZ is the oxygen consumption; ρ is the density; and D is the equivalent diameter of flame area.

2.1.4 Thermal radiation model

$$\mathbf{s} \cdot \nabla I_\lambda(\mathbf{x}, \mathbf{s}) = \kappa_\lambda(\mathbf{x})[I_b(\mathbf{x}) - I_\lambda(\mathbf{x}, \mathbf{s})], \tag{6}$$

where, $I_\lambda(\mathbf{x}, \mathbf{s})$ is the radiation intensity at wavelenght λ; **x** is the position vector; **s** is the unit normal direction vector; $\kappa_\lambda(\mathbf{x})$ is the spectral absortion coefficient; $I_b(\mathbf{x})$ is the source term given by the Planck function and I_b is the radiation blackbody intensity per unit of solid angle.

It was employed a gray gas model for the radiation absorption coefficient (FDS default), a function of gas composition and temperature according to McGrattan *et al.* (2018b). The FDS default mode of gray gas model solver mentioned in McGrattan *et al.* (2018a) was used considering that, in most large scale scenarios, soot is the most important product controling the thermal radiation from the fire and hot smoke. Since radiation spectrum of soot is continuous, that solver mode assumes that the gas behaves as a gray medium. The spectral dependence was then lumped into one absorption coefficient (N = 1) and the source term is given by the blackbody radiation intensity described below:

$$I_b(\mathbf{x}) = \frac{\sigma T(\mathbf{x})^4}{\pi}, \tag{7}$$

where, σ is the Stefan-Boltzmann constant and T is the absolute temperature.

2.1.5 Probit equation

The probality of death due to the exposure to heat radiation from fire is calculated with use of a probit ("probability unit") function. The probit function used for death due to heat radiation is given by VROM (2005a):

$$Pr = -36.38 + 2.56 \ln(Q^{4/3} t), \tag{8}$$

where, Pr is the probit corresponding to the probality of death; Q (W/m^2) is the heat radiation and t(s) is the exposure time, with maximum value of 20 s.

2.2 Simulation parameters

In Cases 1 to 6, the following parameters were specified to the fire simulations:

1. Single mesh (straight due to FDS feature) with the domains defined in Cartesian axes x, y and z as:
   - x axis: -15 m to 15 m;
   - y axis: -15 m to 15 m and;
   - z axis: 0 m to 30 m;
   - each mesh is formed by cubic cells with a 3 cm long edge;
2. Radiative Fraction (fraction of heat generated transmitted in the form of radiation): 0.4;
3. Number of radiation angles used for spatial resolution of Radiation Transport Equation: 100 (FDS default);
4. Emissivity: 1.0;
5. Heat of combustion: 4.45×10^4 kJ/kg;
6. CO yield (yield of CO gas emitted from the fire): 0.011 and;
7. Soot yield (yield of soot emitted from the fire): 0.038.

The value of the radiative fraction corresponds to the value specified for N-Octane in McGrattan *et al.* (2018b). The values of heat of combustion, CO and soot yields (the mass of C0 and smoke/soot produced per mass of fuel burned) were obtained from DiNenno *et al.* (2002).

The dimensions of objects in simulations are described below:

- Case 1 and 2: horizontal cylindrical tank with internal diameter =2.48 m, lenght = 4.14 m, wall thickness = 0.0224 m; above a containment basin with 6 m of lenght and width, wall height = 0.81 m and with wall and floor thickness = 0.2 m;
- Case 3 and 4: vertical cylindrical tank with internal diameter =6.80 m, height = 7.60 m and wall thickness = 0.0224 m;
- Case 5 and 6: containment basin with 6 m of lenght and width, wall height = 0.91 m and with wall and floor thickness = 0.2 m;

The volume of liquid fuel considered was 18 m^3 in Cases 1, 2, 5 and 6 inside the containment basin and; 248.41 m^3 inside the tank in Cases 3 and 4. The fuel volume in the tanks was determined as 80% of the capacity of the tanks. The fluid volume in the containment basin in Cases 5 and 6 was considered the same as of the tanks of Cases 1 and 2.

The wind paramaters when considerated were:

- Case 2: Speed = 2 m/s and direction = 135° (from South East to North West);
- Case 4: Speed = 4 m/s and direction = 0° (from North to South);
- Case 6: Speed = 1 m/s and direction = 0° (from North to South).

2.3 Radiation estimation method

In order to analyse the fire hazards, the radiative heat transfer was computed at several points using the FDS device named "Radiative Heat Flux Gas". In these points, the "Radiative Heat Flux Gas" devices were applied, thus establishing one mesh of evaluation points for the incident radiative heat flux for all simulations. Considering the Cartesian coordinate system with the x, y and z axes, the x and y axes being parallel to the ground and the z axis perpendicular to the ground, the mesh of evaluation points was defined with the following configuration:

1. 22 axis x parallel lines, beginning in $x = -14$ m and ending in $x = 14$ m, in each line, 28 points are equally spaced. The lines are located in $y = -14$ m; -13 m; -12 m; -11 m; -10 m; -9 m -8 m; -7 m; -6 m; -5 m; -4 m; 4 m; 5 m; 6 m; 7 m; 8 m; 9 m; 10 m; 11 m; 12 m; 13 m and 14 m.
2. 7 axis x parallel lines, beginning in $x = -14$ m and ending in $x = -4$ m, in each line, 11 points are equally spaced. The lines are located in $y = -3$ m; -2 m; -1 m; 0 m; 1 m; 2 m e 3 m.
3. 7 axis x parallel lines, beginning in $x = 4$ m and ending in $x = 14$ m, in each line, 11 points are equally spaced. The lines are located in $y = -3$ m; -2 m; -1 m; 0 m; 1 m; 2 m e 3 m.

At each point, the radiation was computed for 26 different directions, simulating the presence of 26 radiometers pointing out each one to a different direction. The directions are symmetrically distributed in order to capture the incident radiation in each one. All simulated radiometers are located at a height of 1.70 m from the ground level. The Figure 1 shows the mesh of evaluation points with "Radiative Heat Flux Gas" devices to Cases 1 and 2, 3 and 4, and 5 and 6 respectively.

3. RESULTS

The six pool fires simulations were runned using FDS to simulate 60 seconds of fire. The Figure 2 shows Cases 1, 3, and 5 (without wind) respectively, at simulation time $t = 30$ s. The Figure 3 shows Cases 2, 4, and 6 (with wind) respectively, at simulation time $t = 30$ s.

The results obtained from FDS for the radiation in the above cases were processed using Matlab program to give the maximum distance reached by the radiative heat flux from pool fire at the levels of interest. The levels of interest are 5 kW/m^2, capable of causing second degree burn, and 9.8 kW/m^2, corresponding to the probit of death probability of 1%, according to Eq. (8). The Matlab program also plotted contour curves of the radiative heat flux from pool fire at the levels of interest when they are reached in the simulation, outside the fire zone.

FDS has extensive validation and verification documentation, including thermal radiation validation with the analytical device used in this work. However, the method used in this work must be validated, considering all specific parameters involved.

The Fig. 4, 5, 6, 7, 8 and 9 show graphics plotted with Matlab to Cases 1, 2, 3, 4, 5 and 6 respectively. For Cases 1, 2, 4, 5 and 6, each dashed circle touches the greatest distance reached by the corresponding thermal radiation intensity of interest. In Case 3 contour curves $Q = 5$ kW/m^2 and 9.8 kW/m^2 were not found and in Case 4 contour curve $Q = 9.8$ kW/m^2 was not found.

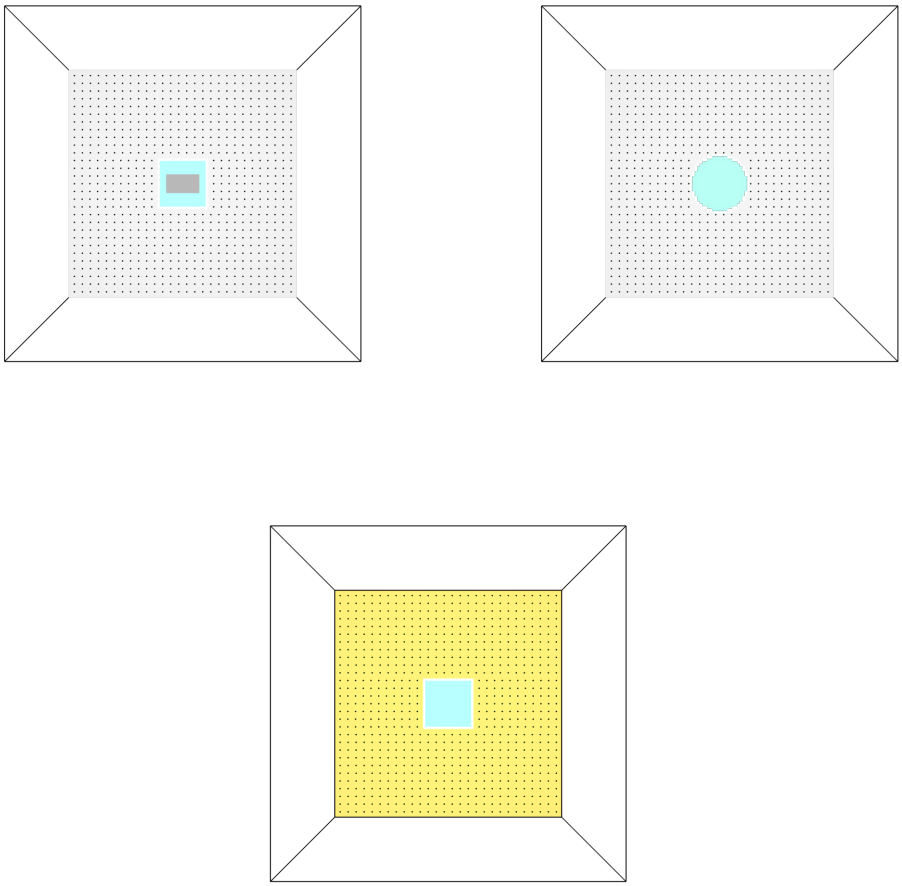

Figure 1. Top view of mesh of evaluation points with "Radiative Heat Flux Gas" devices to Cases 1 and 2 (up left), 3 and 4 (up right), and 5 and 6 (below). The x-axis is horizontal and the y-axis is vertical.

The safety distances from pool fires scenarios using the method adopted to estimate radiative heat flux equal to 5 kW/m^2 and 9.8 kW/m^2 are shown in Tab. 1. These distances are given by the largest distance reached by the corresponding contour curves, measured from the center of the tank or the containment basin, and are shown as dashed circles in Fig. 4, 5, 6, 7, 8 and 9.

Table 1. Distances from pool fires to radiative heat flux of interest.

Scenario	**Fuel Volume(m^3)**	**Wind Speed (m/s)**	**Wind Direction**	**5 kW/m^2**	**9.8 kW/m^2**
Case 1	18.00	0.00	-	10,89 m	8,73 m
Case 2	18.00	2.00	135º	14,87 m	12,26 m
Case 3	248.41	0.00	-	-	-
Case 4	248.41	4.00	0º	11,20 m	-
Case 5	18.00	0.00	-	10,83 m	8,23 m
Case 6	18.00	1.00	0º	12,29 m	9,66 m

Note: measured at 1.70 m of height.

4. CONCLUSIONS

The application of computational fluid dynamics (CFD) for fire modeling and simulation is shown to be a viable and advantageous method for providing more realistic results.

The use of CFD makes it possible to work in detail the influences of geometries, mass transport, amount of movement

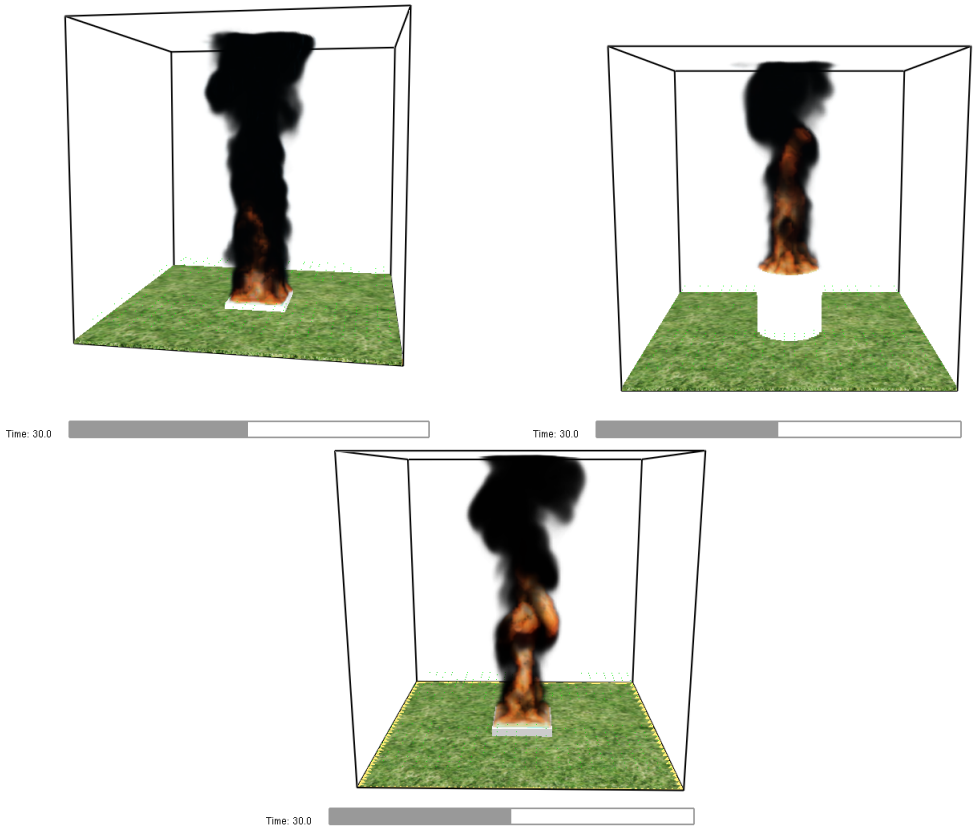

Figure 2. Smoke View figures from pool fire simulations in FDS to Cases 1 (up left), 3 (up right) and 5 (below) without wind at simulation time $t = 30$ s.

and energy in the simulations of the models. The results obtained from the simulations can be processed to provide accurate data on the physical effects prevailing in the areas of interest in the computational domain. The obtained information can be treated mathematically to obtain with considerable degree of precision the levels of intensity of thermal radiation emitted by a fire.

For fire modeling and simulation, the complexity of the modeling, the processing time and the computational demand are, at present, disadvantages for the use of CFD compared to the simplified methods of semi-empirical modeling that have a simpler modeling, small processing time and computational demand.

In the simulation of a model, the smoke generated by the fire and its propagation has a lot of influence on the thermal radiation flux, since the smoke absorbs, scatters, and emits radiation.

The climatic data of the model must consider the worst hypothesis scenario within the probabilities to be considered, due to the fact that they are determinant in the shape of the flames, in the trajectory of the smoke and consequently in the propagation of the thermal radiation.

It is concluded that the use of computational fluid dynamics provides relevant information for the analysis of risk of injury and death of people due to fires in installations that store or process flammable and combustible substances.

5. ACKNOWLEDGEMENTS

The authors would like to acknowledge Rio de Janeiro State Institute of Environment (INEA) and Rio de Janeiro State University (UERJ) the opportunity to do this work, Thunderhead Engineering for providing the free student license for the software Pyrosim, and the financial support from FAPERJ, CNPq and CAPES.

6. REFERENCES

DiNenno, P.J., Drysdale, D., Beyler, C.L., Walton, W.D., Custer, R.L.P., Jr., J.R.H. and Watts, J.M., 2002. *SFPE Handbook of Fire Protection Engineering*. National Fire Protection Association, Quincy, Massachusetts - USA.

Hostikka, S., McGrattan, K. and Hamins, A., 2003. "Numerical modeling of pool fires using LES and finite volume method for radiation". In *Proceedings of the Seventh International Symposium on Fire Safety Science. International*

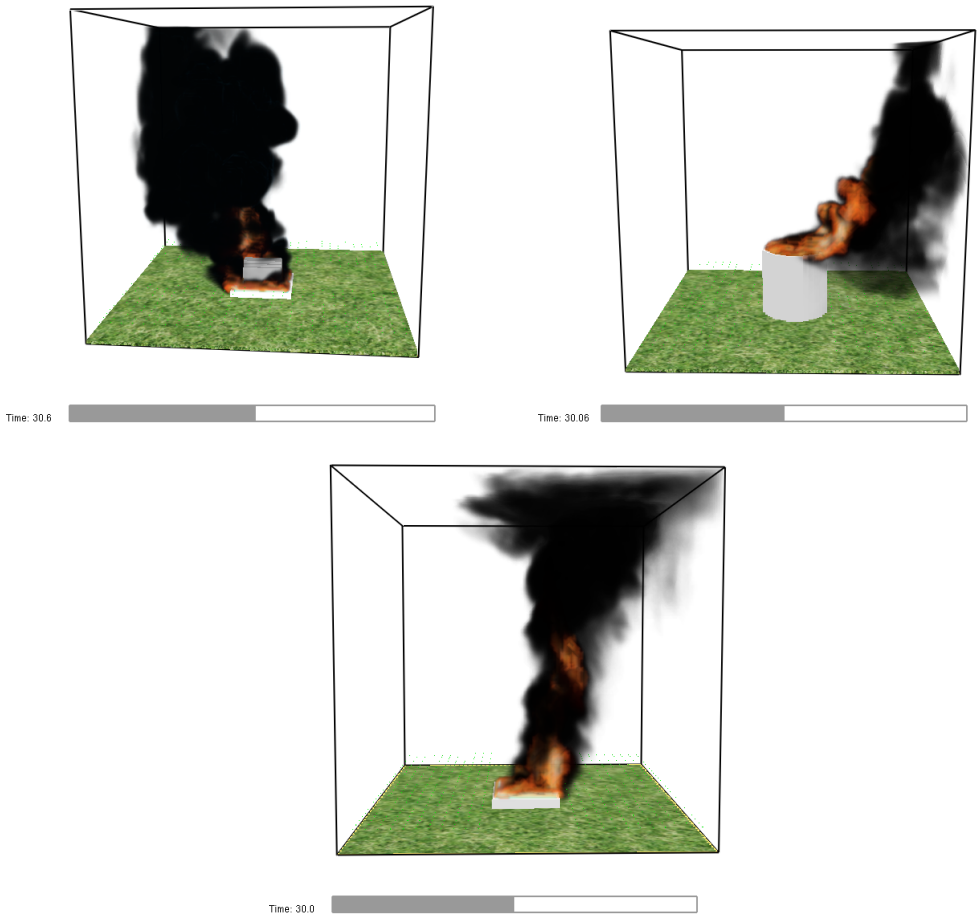

Figure 3. Smoke View figures from pool fire simulations in FDS to Cases 2 (up left), 4 (up right) and 6 (below) with wind at simulation time $t = 30$ s. Views in cases 4 and 6 are rotated to improve visibility.

Association for Fire Safety Science, Pp 383-394.

McGrattan, K., Baum, H.R. and Rehm, R.G., 1998. "Large eddy simulations of smoke movement". *Fire Safety Journal*, Vol. 30, No. 2, pp. 161–178.

McGrattan, K., Hostikka, S., McDermott, R., Floyd, J. and Vanella, M., 2018a. *Fire Dynamics Simulator Technical Reference Guide Volume 1: Mathematical Model*. NIST - National Institute of Standards and Technology and VTT Technical Research Centre of Finland, Gaithersburg, Maryland - USA.

McGrattan, K., Hostikka, S., McDermott, R., Floyd, J. and Vanella, M., 2018b. *Fire Dynamics Simulator User's Guide*. NIST - National Institute of Standards and Technology and VTT Technical Research Centre of Finland, Gaithersburg, Maryland - USA.

Niazi, U.M., Nasif, M.S., Muhammad, M.B. and Imran, M., 2016. "Modelling of pool fire and injury prediction considering different wind speeds and directions in offshore platform". *ARPN Journal of Engineering and Applied Sciences*, Vol. 11, No. 22, pp. 13000–13005.

Silva, M. and Mangiavacchi, N., 2019. "Computional fluid dynamics (CFD) applied to model pool fire and radiation heat flux to injury prediction". In *Proceedings of the 25th International Congress of Mechanical Engineering - COBEM 2019*. Uberlândia, Brazil.

VROM, M.v., 2005a. *Guidelines for Quantitative Risk Assessment - CPR 18E Part One: Establishments - "Purple Book"*. Ministerie van VROM, Nederland.

VROM, M.v., 2005b. *Methods for the Calculation of Physical Effects - CPR 14E - "Yellow Book"*. Ministerie van VROM, Nederland.

7. RESPONSIBILITY NOTICE

The authors are solely responsible for the printed material included in this paper.

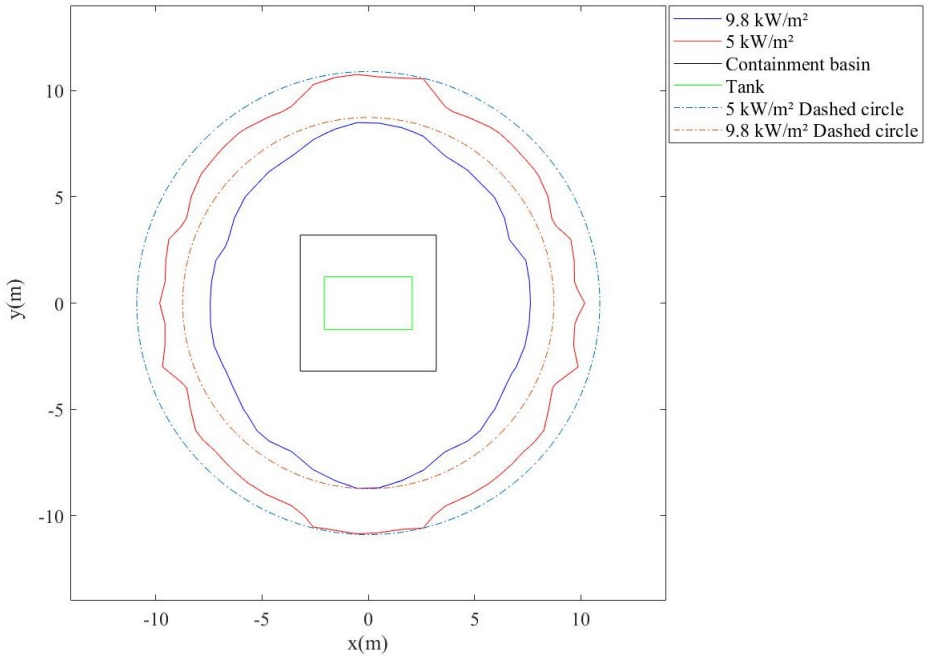

Figure 4. Radiative heat flux contour curves with the corresponding dashed circles to Case 1

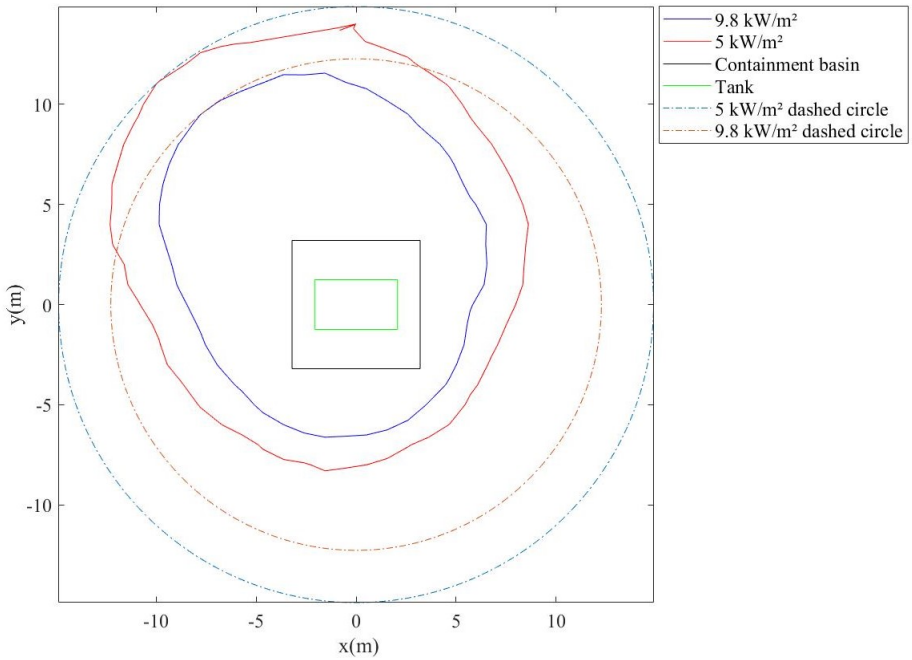

Figure 5. Radiative heat flux contour curves with the corresponding dashed circles to Case 2

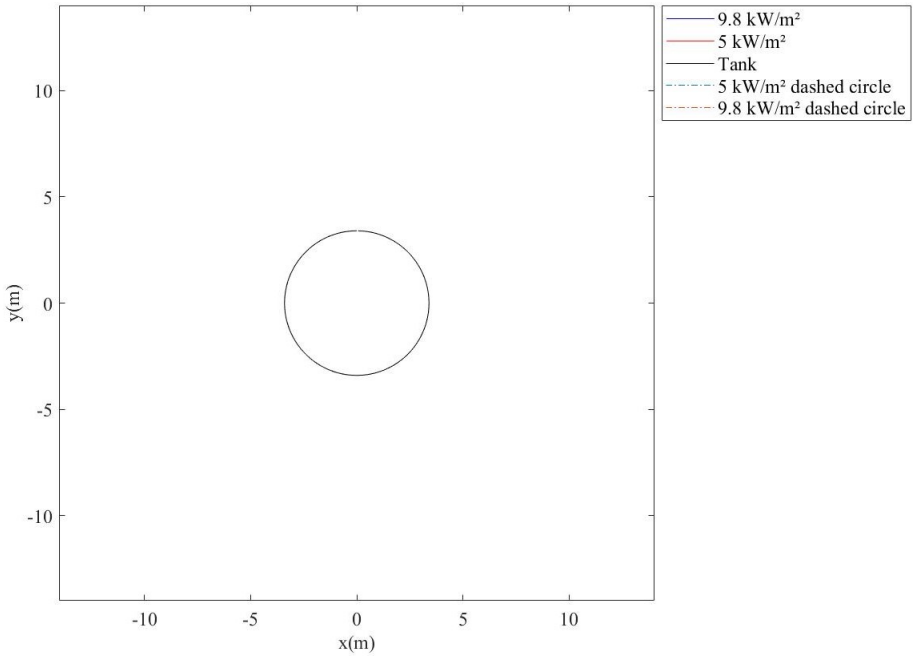

Figure 6. Radiative heat flux contour curves with the corresponding dashed circles not found to Case 3

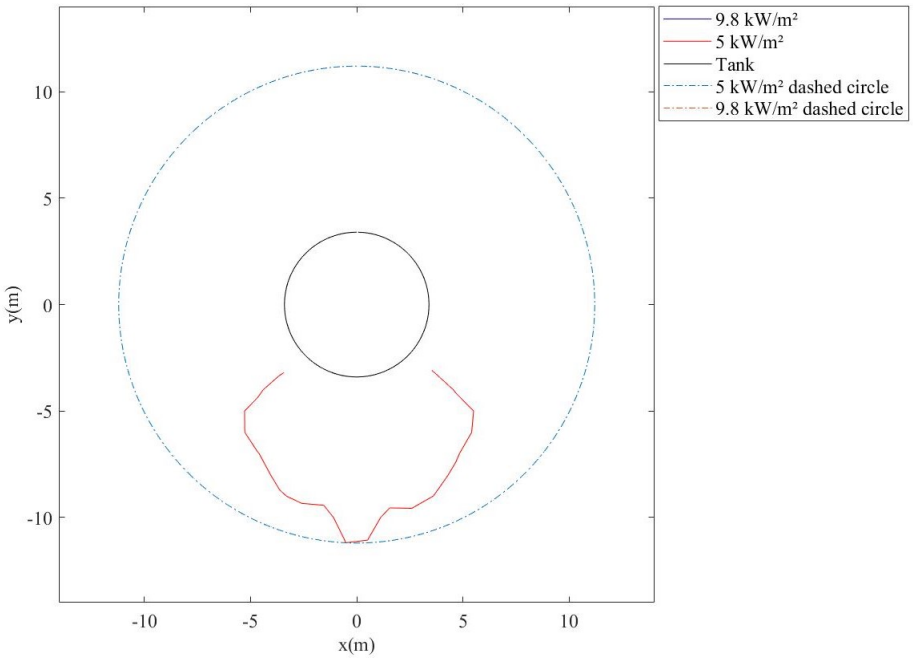

Figure 7. Radiative heat flux contour curve with the corresponding dashed circle only found to 5 kW/m^2 to Case 4

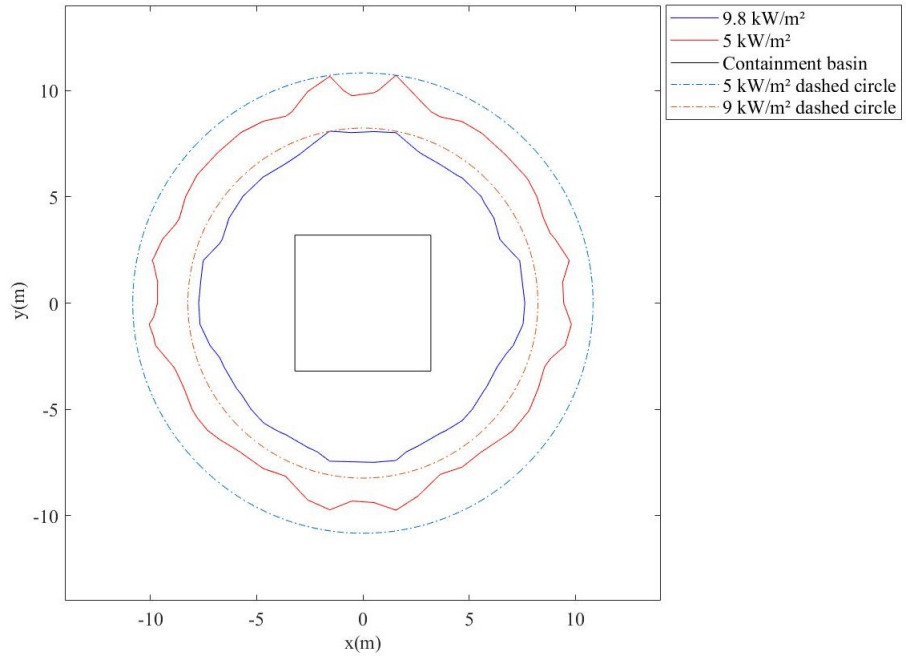

Figure 8. Radiative heat flux contour curves with the corresponding dashed circles to Case 5

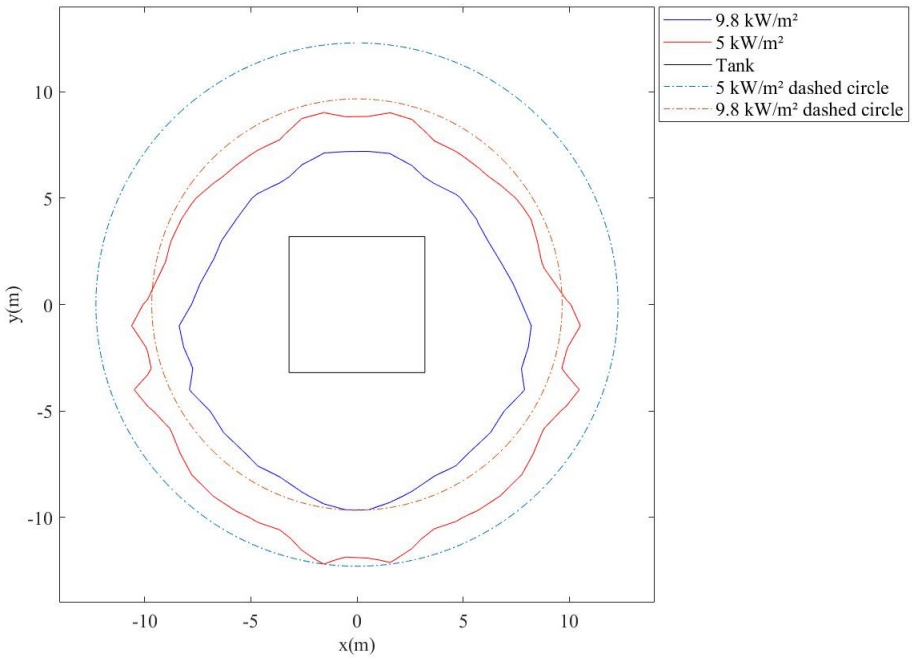

Figure 9. Radiative heat flux contour curves with the corresponding dashed circles to Case 6